Arch. Metall. Mater. **69** (2024), 3, 1115-1122

DOI: https://doi.org/10.24425/amm.2024.150932

A. VAŠKO[1*], V. ZATKALÍKOVÁ[1], M. UHRÍČIK[1], V. KAŇA[2]

# CORROSION RESISTANCE OF AUSTENITIC NiMn-NODULAR CAST IRON IN NaCl SOLUTION

Austenitic nodular cast iron is a versatile material that offers a unique combination of properties, making it suitable for use in a wide range of applications where high strength, ductility, toughness, corrosion resistance and wear resistance are required. This material is commonly used in a variety of applications in the chemical and petrochemical industries, in the automotive and aerospace industries, as well as in marine and offshore applications.

For the experiments, one of the most common austenitic nodular cast irons (alloyed with nickel and manganese) was chosen. The aim of this paper is to evaluate the corrosion resistance of this austenitic nodular cast iron and compare it with other (non-austenitic) types of nodular cast iron (SiMo- and SiCu-type). Corrosion resistance was determined by an exposure immersion test and an electrochemical potentiodynamic polarization test. Both tests were performed in a 3.5% NaCl solution (to simulate seawater) at ambient temperature.

Experimental results prove that austenitic NiMn-nodular cast iron has a higher corrosion resistance than SiMo- and SiCu-nodular cast iron. Moreover, austenitic nodular cast iron has better plastic properties (higher elongation and absorbed energy) but worse strength and fatigue properties (lower tensile strength, hardness and fatigue limit) than the other types of nodular cast iron.

*Keywords:* Corrosion; Ni-Resist; austenitic nodular cast iron; EN-GJSA-XNiMn13-7

## 1. Introduction

Austenitic cast iron grades are high-alloy cast irons with lamellar or nodular graphite which have an austenitic matrix as a common feature. Austenitic cast irons have a number of special technological and physical properties that make them interesting for a wide variety of applications: corrosion resistance, scaling resistance, high heat resistance, thermal shock resistance, high ductility, wear and erosion resistance, low-temperature toughness, non-magnetizability and particularly high or low thermal expansion coefficients (depending on the nickel content) [1-3]. Austenitic cast irons are often referred to worldwide as Ni-Resist [4].

The austenitic cast iron grades are described in detail by the European standard STN EN 13835 „Founding – Austenitic cast irons". The standard prescribes the required structure, chemical composition, mechanical and physical properties and areas of application for the different grades. In general, austenitic cast irons have excellent corrosion resistance, but the standard does not prescribe these properties.

To ensure a stable austenitic matrix at low temperatures, after heat treatment and/or under mechanical stress, a high content of austenite-stabilizing elements such as nickel, manganese and copper is required. These elements can be combined according to the following formula for the nickel equivalent proposed for nodular cast iron [1]:

$$\text{Nickel equivalent} = \%\,\text{Ni} + 2\%\,\text{Mn} + \%\,\text{Cr} > 23.5\% \quad (1)$$

Chromium dissolved in the matrix has a stabilizing effect on austenite [5].

The corrosion behaviour of austenitic cast iron is different from that of corrosion-resistant steels. In these stainless steels, corrosion resistance is based on the formation of a passive layer due to the chromium content of at least 12% dissolved in the austenitic matrix; nickel and other alloying elements have an effect only at higher contents than in the usual types of steel [6,7]. In the case of austenitic cast irons, the chromium content is not sufficient for the formation of a passive layer, but the resistance is based on the inherent resistance of the nickel-containing matrix or the formation of protective layers from corrosion products. All other alloying elements, especially chromium, are then involved in the formation of the protective layer. Therefore, with increasing contents of nickel and chromium, the resistance

[1] UNIVERSITY OF ŽILINA, FACULTY OF MECHANICAL ENGINEERING, DEPARTMENT OF MATERIALS ENGINEERING, ŽILINA, SLOVAKIA
[2] BRNO UNIVERSITY OF TECHNOLOGY, FACULTY OF MECHANICAL ENGINEERING, DEPARTMENT OF FOUNDRY ENGINEERING, BRNO, CZECH REPUBLIC
* Corresponding author: alan.vasko@fstroj.uniza.sk

increases in most cases. For this reason, the surface of castings made of austenitic cast iron does not remain permanently silver-metallic and shiny like stainless steel, even when exposed to air, but is covered with a kind of patina. This is not a material defect, but typical for this material [8].

The surface corrosion rate of austenitic cast irons is generally higher than that of corrosion-resistant steels. On the other hand, there is no danger of breaking through the thin passive layer and the occurrence of local corrosion, such as pitting or crevice corrosion, of which stainless steels are so feared [9-11].

The shape of the graphite has practically no influence on the corrosion behaviour, so the corresponding grades with lamellar and nodular graphite behave in the same way. Austenitic cast iron with nodular graphite is preferred today over austenitic cast iron with lamellar graphite because of its higher strength [12].

Austenitic cast iron has relatively good resistance to atmospheric corrosion, although it is covered with a layer of rust. However, unlike the behaviour of unalloyed cast iron or steel, this protects the underlying material from further attack. The corrosion resistance of austenitic cast iron in seawater and salt solutions is significantly better than that of unalloyed cast iron or casting steel. Austenitic cast iron is up to ten times more resistant than unalloyed nodular cast iron. Therefore, one of the most important applications of austenitic cast iron are components of equipment and machinery that come into contact with seawater, brackish water, polluted river water and concentrated salts [1,13-15].

Some technical books and papers deal with the comparison of the corrosion resistance of austenitic cast irons and stainless steels (in the case of surface corrosion, austenitic cast steel is more resistant in most cases but is susceptible to pitting corrosion) or compare the corrosion behaviour of austenitic cast irons with that of unalloyed cast irons or unalloyed cast steels [16-19]. The aim of this paper is to evaluate the corrosion resistance of austenitic NiMn-nodular cast iron and to compare it with alloyed non-austenitic types of nodular cast iron (SiMo- and SiCu-). These nodular cast irons contain different alloying elements and each of these alloying elements affects the corrosion properties of the cast irons in a different way.

The presence of silicon, copper or molybdenum in nodular cast iron enhances its resistance to oxidation. Silicon reacts with oxygen in the atmosphere and forms an oxide layer (silicon dioxide $SiO_2$) on the surface of cast iron. This layer acts as a protective barrier against further corrosion (it helps to prevent direct contact between the metal and the surrounding environment) and slows down the oxidation process, thus improving the overall corrosion resistance. The addition of other alloying elements, such as copper or molybdenum, in combination with silicon can further enhance the corrosion resistance of nodular cast iron in specific applications or environments [20,21].

## 2. Experimental material and methods

The research was aimed at evaluating the corrosion resistance of austenitic NiMn-nodular cast iron in salt solution and comparing it with other alloyed (non-austenitic) types of nodular cast iron. The basic mechanical properties of the examined cast irons were also evaluated and compared.

For the experiments, austenitic nodular cast iron alloyed with 13% nickel and 7% manganese was chosen. The designation of this nodular cast iron according to STN EN 13835 is EN-GJSA-XNiMn13-7 by symbol and 5.3506 by number. Melting was carried out in an electric induction furnace and subsequently, Y blocks with a wall thickness of 60 mm and a length of 250 mm were cast. The basic charge consisted of steel, pig iron and additives to change the chemical composition, such as carburizer, ferrosilicon, nickel and ferromanganese (TABLE 1). FeSiMg7 modifier and FeSi75 inoculant were used for modification and inoculation. The content of the charging materials was chosen to achieve the required chemical composition and austenitic matrix. TABLE 2 provides information on the required and resulting chemical composition of the melt. The nickel equivalent calculated according to the formula (1) is 26.2%, which ensures a stable austenitic matrix at ambient temperature.

Carbon equivalent was calculated according to the following formula [1,20]:

$$C_E = \% C + 0.33 \cdot \% Si + \\ + 0.047 \cdot \% Ni - 0.0055 \cdot \% Ni \cdot \% Si \qquad (2)$$

TABLE 1

Charge composition of the melt for EN-GJSA-XNiMn13-7 (5.3506)

| Charging raw materials (kg) | | | | | | Modification & inoculation (kg) | | |
|---|---|---|---|---|---|---|---|---|
| **Steel** | **Pig iron** | **Carburizer** | **FeSi75** | **Ni** | **FeMn80** | **Modifier FeSiMg7** | **Inoculant FeSi75** | **Cover plates** |
| 23.5 | 17.5 | 0.7 | 1.7 | 7.8 | 5.5 | 0.7 | 0.4 | 3.0 |

TABLE 2

Required and resulting chemical composition of EN-GJSA-XNiMn13-7 (5.3506)

| | Content of chemical elements (weight %) | | | | | | | | | | | $C_E$ |
|---|---|---|---|---|---|---|---|---|---|---|---|---|
| | **C** | **Si** | **Mn** | **Ni** | **Cr** | **Cu** | **P** | **S** | **Mo** | **Al** | **Mg** | |
| **Required** | max 3.00 | 2.00-3.00 | 6.00-7.00 | 12.0-14.0 | max 0.20 | max 0.50 | max 0.08 | — | — | — | — | — |
| **Real** | 2.634 | 2.177 | 6.365 | 13.45 | 0.061 | 0.038 | 0.035 | <0.015 | 0.024 | 0.026 | 0.094 | 3.82 |

The research included the following experimental methods:

a) metallographic analysis (according to STN EN ISO 945) including automatic image analysis (using NIS Elements software);
b) mechanical tests, i.e.
   – tensile test (according to STN EN ISO 6892-1),
   – impact bending test (according to STN EN ISO 148-1),
   – Brinell hardness test (according to STN EN ISO 6506-1),
   – fatigue tests (according to STN 42 0362) at low-frequency sinusoidal cyclic push-pull loading (stress ratio $R = -1$);
c) corrosion tests in 3.5% NaCl solution (to simulate seawater), i.e.
   – exposure immersion test,
   – electrochemical potentiodynamic polarization test,

both at ambient temperature ($T = 23 \pm 5$°C).

Metallographic analysis and mechanical tests are described in detail in previous paper [22]; this research focuses on corrosion tests.

The exposure immersion test is based on immersing the specimens in a corrosive solution for a period of time. The weight loss of the specimens is determined after removal from the solution and the corrosion rate is defined after recalculation per unit of area and unit of time [23].

Twelve cuboid-shaped specimens were used for the exposure immersion test. The shape and dimensions of the specimens are shown in Fig. 1. The surface of the specimens was prepared by grinding, polishing and finally degreasing with ethanol. Before the test, all specimens were weighed out ($m_1$) using an analytical balance with an accuracy of ±0.000 01 g. A 3.5% NaCl solution was used to simulate seawater. The specimens were suspended from a holder (a glass rod) using insulated wires and immersed in the solution (Fig. 2). They were left in the solution for 1, 2, 4 and 8 weeks. After the required time, three samples were removed from the solution. Subsequently, the specimens were then cleaned (carefully brushed), washed with demineralized water and ethanol, dried up and weighed out ($m_2$) again using the analytical balance. The weight loss was determined as the difference between the weights before and after the test ($\Delta m = m_1 - m_2$). Then, the corrosion rate was calculated from the weight loss during the exposure immersion test, the area of the specimen and the time of the test. The average corrosion rate was determined as the arithmetic mean of the corrosion rates of the three tested specimens [24].

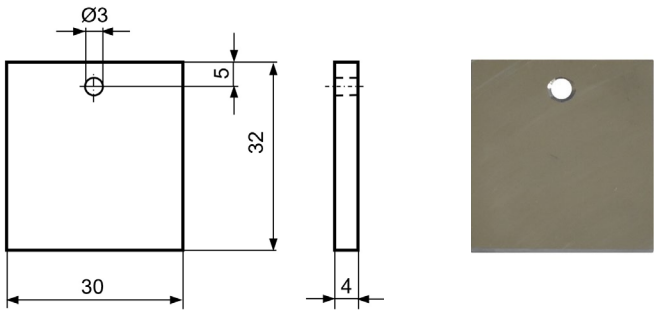


Fig. 1. Specimen for the exposure immersion test

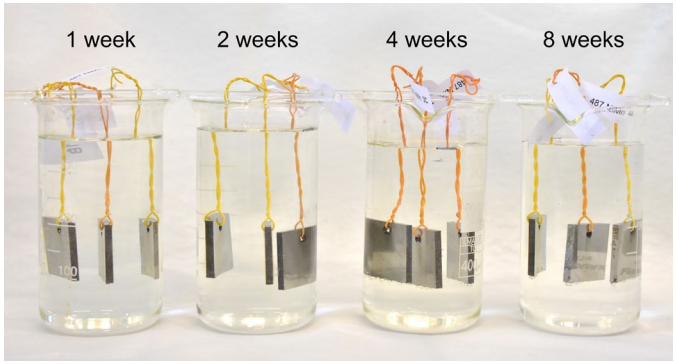


Fig. 2. Procedure of the exposure immersion test

The potentiodynamic polarization test was carried out in a three-electrode corrosion cell (Fig. 3) using a VoltaLab 10 corrosion measuring system with a VSP BioLogic potentiostat. For the potentiodynamic polarization test, the same specimens were used as for the exposure immersion test, the surface of the specimens was prepared in the same way. A specimen with a tested area of 1 cm$^2$ was used as the working electrode. A saturated calomel electrode (SCE) was applied as the reference electrode and a platinum foil as the counter electrode [25,26]. The test was carried out at ambient temperature (23 ± 5°C) in the same solution (3.5% NaCl solution) as the exposure immersion test.

Stabilization of the potential between the specimen and the electrolyte before polarization took 10 minutes. Subsequently, the scan range was set from –0.3 V to +0.2 V versus the open circuit potential and the scan rate was 1 mV/s. Potentiodynamic polarization curves, which express the dependence of current density on potential, were obtained using EC-Lab software. Three measurements were performed on each specimen.

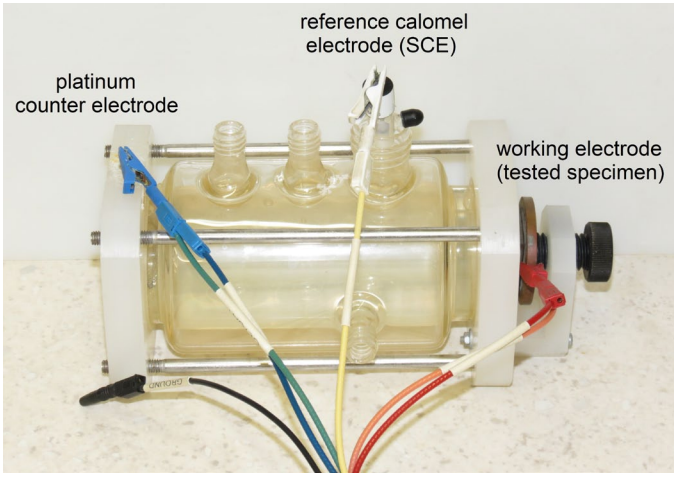


Fig. 3. Three-electrode corrosion cell for potentiodynamic polarization test

Based on the Tafel analysis of the obtained potentiodynamic polarization curves, the corrosion potential $E_{corr}$ and the corrosion current density $i_{corr}$ were determined. The shift of the corrosion potential in the positive direction indicates a higher thermodynamic stability of the metal or alloy. The value of the

TABLE 3

Chemical composition of EN-GJS-X300SiMo4-1 and EN-GJS-X300SiCu4-1.5

| Type of NCI | Content of chemical elements (weight %) | | | | | | | | | | | $C_E$ |
|---|---|---|---|---|---|---|---|---|---|---|---|---|
| | C | Si | Mn | Mo | Cu | P | S | Ni | Cr | Al | Mg | |
| SiMo | 3.021 | 4.094 | 0.376 | 0.938 | 0.115 | 0.026 | 0.032 | 0.059 | 0.084 | 0.027 | 0.039 | 4.381 |
| SiCu | 3.281 | 4.156 | 0.363 | 0.009 | 1.394 | 0.028 | 0.037 | 0.055 | 0.072 | 0.031 | 0.049 | 4.661 |

corrosion current density is directly related to the kinetics of the corrosion process. A lower value of corrosion current density means a lower corrosion rate [24].

To compare the corrosion resistance of austenitic NiMn-nodular cast iron, two other alloyed (non-austenitic) nodular cast irons were used (TABLE 3), namely [27]:

– SiMo-nodular cast iron with a ferritic-pearlitic matrix (designated as EN-GJS-X300SiMo4-1),
– SiCu-nodular cast iron with a pearlitic-ferritic matrix (designated as EN-GJS-X300SiCu4-1.5).

## 3. Experimental results and discussion

The microstructure of NiMn-nodular cast iron is shown in Fig. 4. The specimen has an austenitic matrix and nodular graphite. The austenitic matrix was obtained by adding nickel and manganese. The predominant shape of graphite is a perfectly nodular shape; an imperfectly nodular shape of graphite is rare. The segregation of the main elements dissolved in the solid solution, mainly silicon, manganese and nickel, is shown in the coloured areas of the matrix. The silicon content is highest around the graphitic nodules (beige colour) and lowest in the spaces between these nodules (brown to light blue colour). The segregation of manganese is inverse; the lowest manganese content is near the graphitic nodules. The light blue area also includes impurities and inclusions.

Fig. 5 shows the microstructure of two other alloyed (non-austenitic) nodular cast irons that were used to compare the corrosion resistance of austenitic NiMn-nodular cast iron. SiMo-nodular cast iron has a ferritic-pearlitic matrix (Fig. 5a) and SiCu-nodular cast iron has a pearlitic-ferritic matrix (Fig. 5b).

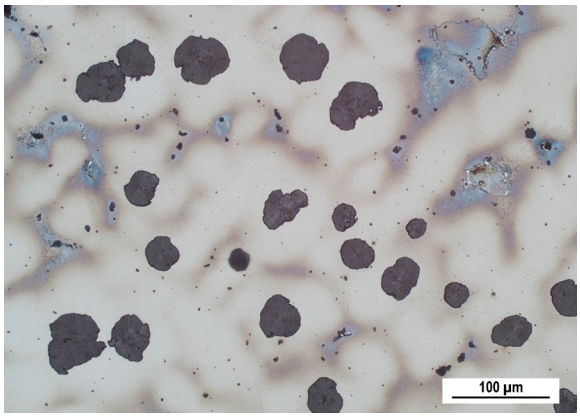


a) austenitic nodular cast iron

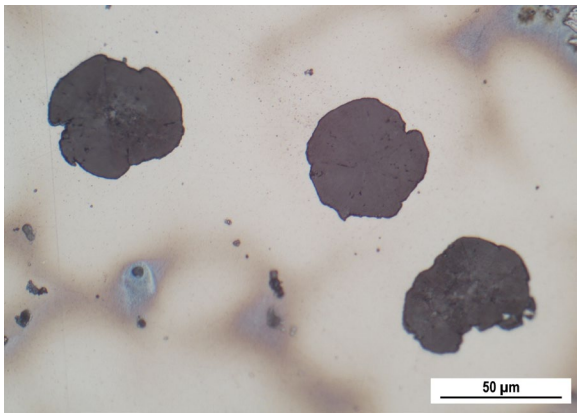


b) detail of microstructure

Fig. 4. Microstructure of austenitic NiMn-nodular cast iron, etched by Kallins 2

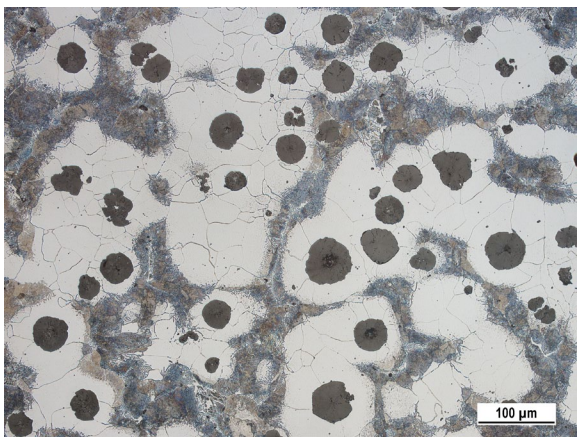


a) ferritic-pearlitic SiMo-nodular cast iron

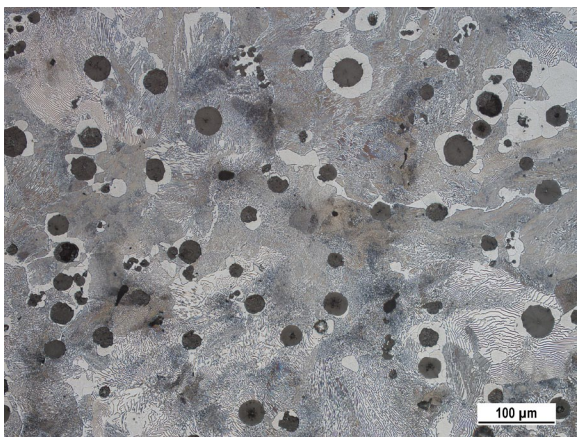


b) pearlitic-ferritic SiCu-nodular cast iron

Fig. 5. Microstructure of non-austenitic nodular cast irons, etched by 3% Nital

SiMo-nodular cast iron should have a significantly higher content of ferrite in the matrix; however, the presence of pearlite is not a mistake. The chemical composition of this cast iron corresponds to the values prescribed by the standard. The appearance of pearlite in the matrix is probably related to the cooling rate of the casting. Pearlite can be removed by heat treatment, but the specimens were left in the cast state. Both non-austenitic nodular cast irons contain graphite predominantly in a perfectly nodular shape.

The microstructure evaluation of all three types of nodular cast iron (NCI) according to the norm is shown in TABLE 4. The results of the microstructure evaluation by automatic image analysis are processed in TABLE 5. Austenitic NiMn-nodular cast iron has a lower shape factor, a larger size of graphite and a smaller count of graphitic nodules compared to the non-austenitic nodular cast irons. SiMo-nodular cast iron has a higher content of ferrite than SiCu-nodular cast iron (due to the pearlitizing effect of copper) and the highest content of graphite. The various chemical compositions of the melts are responsible for the different microstructures.

The shape factor (to express the shape of the graphite) was calculated according to the following formula [28,29]:

$$S = 4\pi A/P^2 \tag{3}$$

where $A$ is an area and $P$ is a perimeter of graphitic particles.

TABLE 4

Microstructure evaluation according to the norm

| Type of NCI | Microstructure (according to STN EN ISO 945) |
|---|---|
| NiMn | 80%VI6 + 20%V6 |
| SiMo | 90%VI6 + 10%V6 – Fe80 |
| SiCu | 90%VI6/7 + 10%V6 – Fe15 |

The mechanical properties of all three types of nodular cast iron (NCI) are shown in TABLE 6. For austenitic NiMn-nodular cast iron, the values of the mechanical properties prescribed according to the norm are listed first, and the measured mechanical properties are given in the next line. The last two lines show the measured mechanical properties of non-austenitic nodular cast irons. Austenitic NiMn-nodular cast iron has a lower yield strength $R_{p0,2}$, tensile strength $R_m$, hardness HBW and fatigue strength $\sigma_c$ compared to non-austenitic nodular cast irons, but significantly higher elongation $A$ and absorbed energy $K0$ (measured on the specimen without a notch). The different mechanical properties are related to the various microstructures of nodular cast irons, especially the character of the matrix, but also to the shape, size and count of graphitic nodules. Silicon has the greatest influence on the increase in strength properties, but plastic properties decrease with increasing content of silicon.

The corrosion resistance of nodular cast irons was evaluated by exposure immersion test and electrochemical potentiodynamic polarization test.

During the exposure immersion test, all specimens were attacked by more or less uniform electrochemical corrosion. In the case of SiMo- and SiCu-nodular cast iron, already after 1 week of exposure in a 3.5% NaCl solution, the entire surface of the specimens was covered with reddish iron oxides as a result of leaching and oxidation of iron ($Fe \rightarrow Fe^{2+} + 2e^{-}$). This form of damage indicates a rapid corrosion process. The corrosion process of austenitic NiMn-nodular cast iron took place significantly slower than in the case of non-austenitic nodular cast irons. An example of corrosion damage on the surface of the specimens after 4 weeks is shown in Fig. 6. The corrosion surfaces of SiMo- and SiCu-nodular cast irons with a matrix formed by ferrite and pearlite are similar; the corrosion products on these specimens are significantly more massive than on the specimen of austenitic NiMn-nodular cast iron. The presence of nickel in austenitic cast iron contributes to increased corrosion resistance in an environment containing NaCl. In addition, nickel acts synergistically with other elements of austenitic NiMn-cast iron, such as manganese (Mn). Together, these components improve corrosion resistance, thereby protecting the material from the effects of the NaCl solution.

The results of the exposure immersion test in 3.5% NaCl solution (after 1, 2, 4 and 8 weeks) for austenitic NiMn-nodular

TABLE 5

Microstructure evaluation by automatic image analysis

| Type of NCI | Shape factor of graphite | Equivalent diameter of graphite (μm) | Count of graphitic nodules ($mm^{-2}$) | Content of graphite (%) | Content of ferrite (%) |
|---|---|---|---|---|---|
| NiMn | 0.72 | 36.3 | 78.1 | 9.4 | — |
| SiMo | 0.88 | 31.2 | 122.8 | 10.2 | 59.4 |
| SiCu | 0.84 | 24.3 | 172.4 | 9.3 | 19.7 |

TABLE 6

Mechanical properties

| Type of NCI | $R_{p0.2}$ (MPa) | $R_m$ (MPa) | $A$ (%) | $K0$ (J) | HBW 10/3000/10 | $\sigma_c$ (MPa) |
|---|---|---|---|---|---|---|
| NiMn (norm) | 210-260 | 390-470 | 15-18 | — | 120-150 | — |
| NiMn | 237.7 | 475.3 | 29.0 | 197.3 | 138.7 | 150 |
| SiMo | 515.3 | 573.9 | 1.4 | 11.3 | 213.7 | 210 |
| SiCu | 631.1 | 652.7 | 0.7 | 8.0 | 247.3 | 270 |

a) NiMn-NCI b) SiMo-NCI c) SiCu-NCI

Fig. 6. Corrosion on the surface of the specimens after 4 weeks

TABLE 7

Results of the exposure immersion test in 3.5% NaCl solution (after 1, 2, 4 and 8 weeks)

| Type of NCI | Specimen No. | Weight before test $m_1$ (g) | Weight after test $m_2$ (g) | Weight loss $\Delta m = m_1 - m_2$ (g) | Corrosion rate (g m$^{-2}$ day$^{-1}$) | Average corosion rate (g m$^{-2}$ day$^{-1}$) |
|---|---|---|---|---|---|---|
| NiMn | 1A | 26.53811 | 26.51899 | 0.01912 | 0.56009 | 0.54711 |
| | 1B | 26.05005 | 26.03071 | 0.01934 | 0.56654 | |
| | 1C | 25.03655 | 25.01898 | 0.01757 | 0.51469 | |
| | 2A | 31.48727 | 31.44988 | 0.03739 | 0.54764 | 0.49091 |
| | 2B | 25.49266 | 25.45996 | 0.03270 | 0.47895 | |
| | 2C | 28.67297 | 28.64251 | 0.03046 | 0.44614 | |
| | 4A | 25.14708 | 25.09888 | 0.04820 | 0.47065 | 0.48852 |
| | 4B | 26.17339 | 26.12245 | 0.05094 | 0.49741 | |
| | 4C | 25.74699 | 25.69604 | 0.05095 | 0.49750 | |
| | 8A | 25.97482 | 25.90760 | 0.06722 | 0.50123 | 0.48667 |
| | 8B | 26.81994 | 26.75602 | 0.06392 | 0.47662 | |
| | 8C | 27.86295 | 27.79829 | 0.06466 | 0.48214 | |

cast iron are given in TABLE 7. First, the weight of the specimens before the test and after the required time of the test was measured, then the weight loss was determined and the corrosion rate was calculated from it. The average corrosion rate was determined as the average value of three measurements.

The results of the exposure immersion test for all three types of nodular cast iron (NCI) are shown in Fig. 7, which expresses the dependence of the average corrosion rate on the test duration. In all three nodular cast irons, the average corrosion rate (recalculated per 1 day) decreases slightly with increasing exposure time. These results of the test correspond to the knowledge that the corrosion rate initially (the first days) increases sharply because a layer of corrosion products is formed, and with increasing exposure time, the corrosion rate gradually decreases [1]. Austenitic NiMn-nodular cast iron has a significantly lower average corrosion rate in salt water compared to non-austenitic nodular cast irons. SiMo-nodular cast iron has approximately 2.7 times higher corrosion rate and SiCu-nodular cast iron has 2.9 times higher corrosion rate than austenitic NiMn-nodular cast iron.

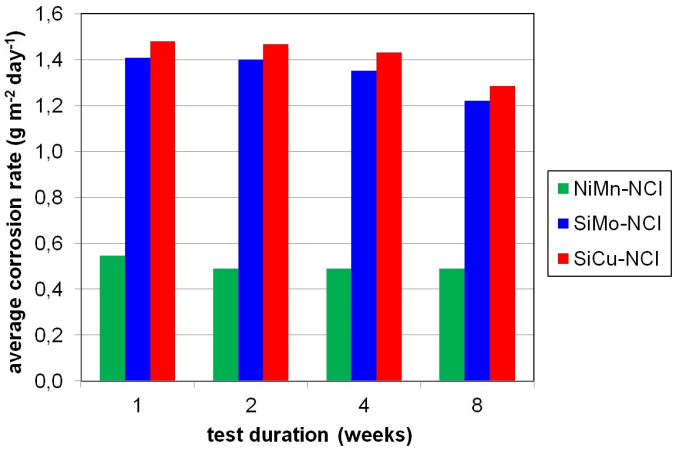


Fig. 7. Dependence of the average corrosion rate on the test duration

The results of the potentiodynamic polarization test for all three types of nodular cast iron (NCI) are shown in Fig. 8, which expresses the dependence of the current density i on the potential E.

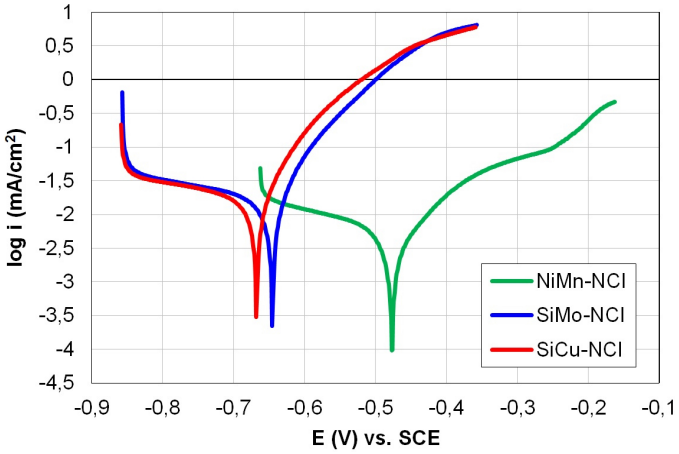


Fig. 8. Potentiodynamic polarization curves (dependence of the current density i on the potential *E*)

The corrosion potential $E_{corr}$, corrosion current density $i_{corr}$ and corrosion rate (recalculated per year) were determined from the polarization curves using Tafel analysis (TABLE 8). Austenitic NiMn-nodular cast iron has a higher corrosion potential and a lower corrosion current density compared to non-austenitic nodular cast irons. The shift of the corrosion potential in the positive direction indicates a higher thermodynamic stability of austenitic NiMn-nodular cast iron. A lower value of corrosion current density means a lower corrosion rate of austenitic NiMn-nodular cast iron. Austenitic NiMn-nodular cast iron has a significantly lower corrosion rate (recalculated per year) compared to non-austenitic nodular cast irons. SiMo-nodular cast iron has an approximately 2.7 times higher corrosion rate and SiCu-nodular cast iron has a 3 times higher corrosion rate than austenitic NiMn-nodular cast iron. Taking into account that the exposure immersion test and the electrochemical potentiodynamic polarization test are independent and carried out under different conditions, the calculated values of corrosion rate $v_{corr}$ correspond to the values of the average corrosion rate determined from the weight loss during the exposure immersion test.

TABLE 8

Electrochemical parameters determined by Tafel analysis

| Type of NCI | $E_{corr}$ (V) | $i_{corr}$ (μA cm$^{-2}$) | $v_{corr}$ (mm year$^{-1}$) |
|---|---|---|---|
| NiMn | –0.476 | 2.660 | 0.031 |
| SiMo | –0.645 | 7.207 | 0.084 |
| SiCu | –0.668 | 8.117 | 0.094 |

Based on both tests, it can be concluded that the corrosion resistance of austenitic NiMn-nodular cast iron in a 3.5% NaCl solution is significantly higher than the resistance of the other two tested types of nodular cast iron. These alloyed (non-austenitic) nodular cast irons corrode intensively in seawater and they should not be used in this environment for long-term applications.

## 4. Conclusion

Due to its chemical composition and microstructure, austenitic NiMn-nodular cast iron has different mechanical properties and corrosion resistance compared to non-austenitic nodular cast irons. These differences can be summarized in the following points:

- Austenitic NiMn-nodular cast iron has worse strength and fatigue properties (lower yield strength, tensile strength, hardness and fatigue strength) but significantly better plastic properties (higher elongation and absorbed energy) than non-austenitic nodular cast irons.
- The exposure immersion test shows that in all three nodular cast irons, the average corrosion rate in seawater initially increases sharply before a layer of corrosion products is formed and then slowly decreases with increasing exposure time. However, austenitic NiMn-nodular cast iron has a significantly lower average corrosion rate compared to non-austenitic cast irons.
- Electrochemical potentiodynamic polarization test shows that austenitic NiMn-nodular cast iron has a higher thermodynamic stability and a significantly lower corrosion rate compared to non-austenitic cast irons.
- Austenitic NiMn-nodular cast iron has 2.7 to 3 times higher corrosion resistance in seawater than the other 2 tested nodular cast irons (compared to unalloyed nodular cast irons, the corrosion resistance would be even higher). This nodular cast iron is suitable for various applications that come into contact with seawater, brackish water, polluted river water and concentrated salts.

**Acknowledgement**

The research has been supported by the Culture and Educational Grant Agency of Ministry of Education, Science, Research and Sport of Slovak Republic, grant projects KEGA No. 009ŽU-4/2023 and 004ŽU-4/2023.

## REFERENCES

[1] K. Röhrig, Konstruieren + Giessen, **29** (2), 2-33 (2004).
[2] Ch. Bartels, R. Gerhards, H. Hanselka, K. Herfurth, H. Kaufmann, W. Kleinkröger, M. Lampic, H. Löblich, W. Menk, G. Pusch, T. Schmidt, K. H. Schütt, P. Tölke, E. P. Warnke, Konstruieren + Giessen **32** (2), 1-101 (2007).
[3] S. Franke, Giesserei-Lexikon, Schiele & Schön, Berlin, Germany (2019).
[4] Properties and applications of Ni-resist and ductile Ni-resist alloys. A practical guide to the use of nickel-containing alloys, No. 11018, Nickel Institute, 1-62 (2022).
[5] V. Kaňa, Slévárenství **65** (1-2), 6-11 (2017).
[6] Corrosion resistance of the austenitic chromium-nickel stainless steels in atmospheric environments. A practical guide to the use of nickel-containing alloys, No. 318, Nickel Institute, 1-13 (2022).

[7] Corrosion resistance of the austenitic chromium-nickel stainless steels in chemical environments. A practical guide to the use of nickel-containing alloys, No. 2828, Nickel Institute, 1-19 (2022).
[8] K. Röhrig, Konstruieren + Giessen **18** (3), 4-29 (1993).
[9] T. Liptáková, Point corrosion of stainless steels, ESIS, Žilina (2009).
[10] T. Liptáková, D. Kajánek, F. Pastorek, V. Zatkalíková, Corrosion properties of selected metals under conditions of their use, EDIS, Žilina (2022).
[11] J. Dziková, D. Kajánek, F. Nový, F. Pastorek, Corrosion of metallic materials, EDIS, Žilina (2021).
[12] Nickel SG-iron – engineering properties. A practical guide to the use of nickel-containing alloys, No. 4077, Nickel Institute (2022).
[13] H.M. Shalaby, S. Attari, W.T. Riad, V.K. Gouda, Corrosion **48** (3), 206-217 (1992).
[14] B. Todd, P. A. Lovett, Marine engineering practice, Vol. 1, Institute of Marine Engineers (1983).
[15] J. C. Rolands, B. Angell, Corrosion for marine and offshore engineers. Institute of Marine Engineering, Science & Technology (2020).
[16] ASM Handbook, Vol. 13A Corrosion: Fundamentals, testing and protection, ASM International (2003).
[17] ASM Handbook, Vol. 13B Corrosion: Materials, Corrosion of cast irons, ASM International (2005).
[18] ASM Handbook, Vol. **1A** Cast iron science and technology, Corrosion of cast irons. ASM International (2017).
[19] M. Schütze, M. Roche, R. Bender, Corrosion resistance of steels, nickel alloys, and zinc in aqueous media: Waste water, seawater, drinking water, high-purity water. Wiley (2015).
[20] Ductile Iron Handbook, American Foundrymen's Society, Des Plaines, Illinois (1993).
[21] M. Stawarz, P.M. Nuckowski, Materials **15** (9), 3225 (2022).
[22] A. Vaško, M. Uhríčik, V. Kaňa, Archives of Metallurgy and Materials **68** (2), 563-569 (2023).
[23] R. Baboian, Corrosion tests and standards: Application and interpretation. ASTM, Philadelphia (2005).
[24] B. Hadzima, T. Liptáková, Basics of electrochemical corrosion of metals. EDIS, Žilina (2008).
[25] R.W. Revie, H.H. Uhlig, Corrosion and corrosion control: An introduction to corrosion science and engineering. John Wiley & Sons, New Jersey (2008).
[26] P. Pedeferri, Corrosion science and engineering, Springer (2018).
[27] A. Vaško, V. Zatkalíková, V. Kaňa, CzOTO 2020, **2** (1), 191-198 (2020).
[28] P. Skočovský, A. Vaško, Quantitative evaluation of structure of cast irons. EDIS, Žilina (2007).
[29] P. Kopas, M. Vaško, M. Handrik, Applied Mechanics and Materials **474**, 285-290 (2014).